Pure Appl. Chem., Vol. 78, No. 6, pp. 1117–1125, 2006.
doi:10.1351/pac200678061117
© 2006 IUPAC

Carbon nanotubes by plasma-enhanced chemical vapor deposition*

Martin S. Bell[1], Kenneth B. K. Teo[1,‡], Rodrigo G. Lacerda[1], W. I. Milne[1], David B. Hash[2], and M. Meyyappan[2]

[1]Engineering Department, University of Cambridge, Cambridge CB2 1PZ, UK; [2]Center for Nanotechnology, NASA Ames Research Center, Moffett Field, CA 94035, USA

Abstract: This paper presents the growth of vertically aligned carbon nanotubes by plasma-enhanced chemical vapor deposition (PECVD) using Ni catalyst and C_2H_2/NH_3 feedstock. The role of plasma in aligning the carbon nanotubes during growth is investigated both experimentally and computationally, confirming that the field in the plasma sheath causes the nanotubes to be aligned. Experiments using a plasma analyzer show that C_2H_2 is the dominant precursor for carbon nanotube growth. The role of NH_3 in the plasma chemistry is also investigated, and experimental results show how the interaction between NH_3 and the C_2H_2 carbon feedstock in the gas phase explains the structural variation in deposited nanotubes for differing gas ratios. The effects of varying the plasma power during deposition on nanotube growth rate is also explored. Finally, the role of endothermic ion-molecule reactions in the plasma sheath is investigated by comparing measured data with simulation results.

Keywords: plasma; PECVD; glow discharge; carbon; nanotubes.

INTRODUCTION

Carbon nanotubes have attracted great interest among researchers since their discovery [1]. Their physical and electronic properties, combined with their chemical inertness, make them potentially useful for applications as diverse as electron-field emitters, nanoelectrodes, filter media, and superhydrophobic surfaces.

In this article, we report on some of the fundamental chemical and physical processes responsible for the deposition of well-aligned carbon nanotubes by plasma enhanced chemical vapor deposition (PECVD).

PRODUCTION OF CARBON NANOTUBES

There are a number of known methods for producing carbon nanotubes. Between them it is possible to produce nanotubes with differing properties and in different forms. The most common methods used for the production of nanotubes are arc discharge [2], laser vaporization [3], and chemical vapor deposition (CVD). Our interest lies mainly in the area of electronic device applications, for which CVD is particularly suitable as it allows the location of nanotubes to be precisely controlled. The carbon source

*Paper presented at the 17th International Symposium on Plasma Chemistry (ISPC 17), Toronto, Ontario, Canada, 7–12 August 2005. Other presentations are published in this issue, pp. 1093–1298.
‡Corresponding author

is a hydrocarbon gas, which dissociates either thermally (thermal CVD) or in the presence of a plasma (PECVD) aided by a transition-metal catalyst. The self-assembly of nanotubes is facilitated by catalyst nanoparticles deposited on the substrate surface which seed the nanotube growth, determining both the location and diameter of the deposited nanotubes. Silicon substrates are typically used in electronic applications as it is amenable for device fabrication using standard semiconductor manufacturing tools.

The catalyst takes the form of a thin film of transition metal (Fe, Ni, Co, or Mo), which may be applied chemically from a solution containing the catalyst or directly by using techniques such as thermal evaporation, ion beam sputtering, or magnetron sputtering. When heat is subsequently applied to the substrate, the increased surface mobility of the catalyst atoms causes the metal film to coalesce into nanoclusters [4]. In order to prevent a chemical reaction between the catalyst and substrate when heat is applied, a thin diffusion barrier of SiO_2, TiN, or indium tin oxide is deposited onto the Si substrate before the metal catalyst layer is deposited. The catalyst layer can be patterned using conventional lithography, which then results in highly localized growth of carbon nanotubes.

In order to prevent the deposition of amorphous carbon ("a-C"), which inhibits the formation of nanotubes by poisoning the growth catalyst and can also cause short circuits on the substrate surface, the carbon source (typically, C_2H_2 or CH_4) is combined with a hydrogen-rich gas (typically, NH_3 or H_2), which produces reactive species in the plasma to remove any excess carbon.

Thermal CVD requires temperatures of 700–1000 °C and has two disadvantages. Firstly, the high temperature rules out the use of some desirable substrate materials (e.g., glass). Secondly, the nanotubes produced are not just randomly oriented; they are also not perfectly straight. PECVD overcomes both of these problems. Energy in the plasma replaces some of the heat energy, allowing gas dissociation and nanotube formation to take place at lower temperatures (600–700 °C), and the electric field in the plasma aligns the nanotubes during growth [5]. There are a number of different techniques available for creating the plasma. These include radio frequency PECVD, microwave PECVD, inductively coupled PECVD, and dc glow discharge PECVD. Figure 1 illustrates the difference between nanotubes deposited with and without a plasma. The conditions in the two cases are identical except for the presence of a dc glow discharge plasma in the case of Fig. 1b. In the purely thermal CVD case, the resultant nanotubes are curly and nonaligned, whereas in the PECVD case, the resultant nanotubes are straight and aligned vertically.

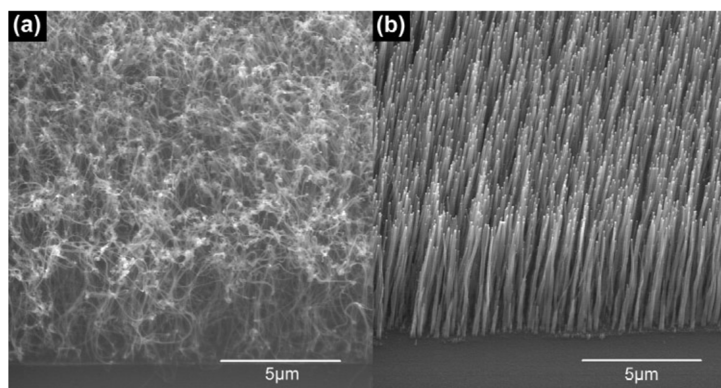

Fig. 1 Deposition (a) without and (b) with plasma.

PROPERTIES OF GLOW DISCHARGE PLASMA

We have seen the effect of the plasma in producing aligned nanotubes and propose that it is the electric field in the plasma sheath which gives rise to the alignment of the nanotubes during growth. In order to investigate the magnitude and extent of this field, a cylindrical Langmuir probe (0.5-mm-radius wire, 5 mm in exposed length) was inserted into a glow discharge plasma under typical deposition conditions. Carbon nanotubes were deposited using dc glow discharge PECVD setup with the substrate located on a resistively heated graphite stage, which also acts as the cathode for the plasma discharge. C_2H_2 was used as the carbon feedstock gas for our carbon nanotube growth, and NH_3 was added to help prevent formation of a-C. NH_3 made up around 17 % of the total gas flux. The gases were fed into the chamber through a showerhead that acted as an anode for the plasma discharge. Negative 600 V was applied to the heated cathode (on which the substrate sits) to generate the plasma glow discharge. The heaters were used to maintain a temperature of around 700 °C.

The voltage variation in a typical dc glow discharge plasma is depicted horizontally in Fig. 2a. The plasma has potential V_p in the glow region. A sheath, extending distance S, is formed close to the cathode, which is the substrate stage. It is the field within this sheath that causes the nanotubes to align during growth. The *I–V* characteristic of the probe was measured and is shown in Fig. 2b.

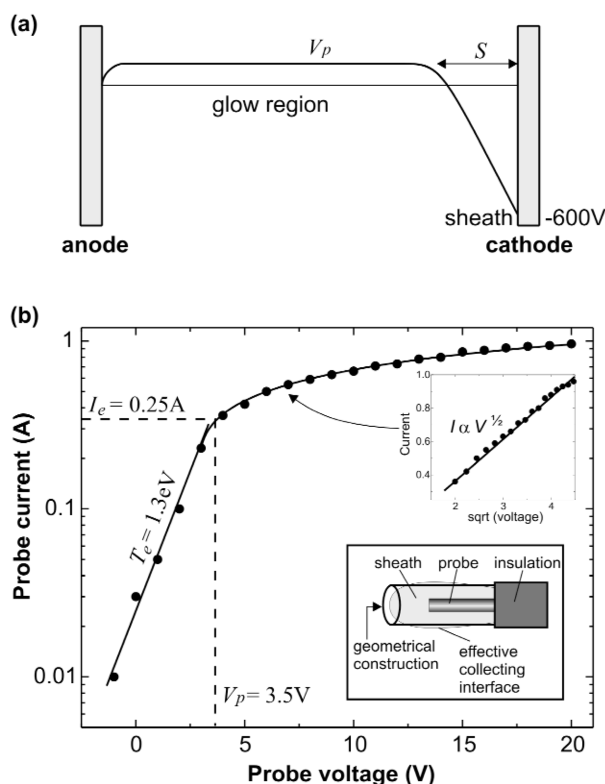

Fig. 2 (a) Typical voltage variation in a dc glow discharge plasma, and (b) *I–V* characteristics of a cylindrical wire Langmuir probe (inset) placed inside the plasma.

A sheath formed around the probe. The collection area was approximated to be a cylinder 3 times the radius of the probe (i.e., $r = 0.15$ cm) and extending twice its length (i.e., $l = 1$ cm) as depicted, giving a total exposed area A of $(\pi r^2 + 2\,\pi rl) = 10^{-4}$ m^2. The probe electron current I_e is given by:

$$I_{\mathrm{e}} = \frac{Ane\overline{c}_{\mathrm{e}}}{4}, \text{ where the mean speed of an electron, } \overline{c}_{\mathrm{e}} = \sqrt{\frac{8kT_{\mathrm{e}}}{\pi m_{\mathrm{e}}}} \quad (1,2)$$

n = electron density, e = electronic charge, k = Boltzmann's constant, T_{e} = electron temperature in K, and m_{e} = electronic mass.

As well as the electron current, there is a corresponding ion current, however, as ion mass is much greater than electronic mass, the mean ion speed and hence the ion current is negligible and the probe current I is approximately equal to I_{e}. If a voltage V of less than the plasma potential V_{p} is applied to the probe, the electrons experience a retarding potential ($V_{\mathrm{p}} - V$). The equation for I must, therefore, be amended to reflect that only those electrons with sufficient energy to overcome the retarding potential can contribute. The net current to the probe can, therefore, be expressed as

$$I \approx I_{\mathrm{e}} \exp\left[-\frac{e\left(V_{\mathrm{p}} - V\right)}{kT_{\mathrm{e}}}\right], \text{ or } \ln\left(I\right) = \ln\left(I_{\mathrm{e}}\right) - \frac{eV_{\mathrm{p}}}{kT_{\mathrm{e}}} + \frac{e}{kT_{\mathrm{e}}}V \quad (3)$$

A plot of ln (I) vs. V for the probe is shown in Fig. 2b. A straight line has been fitted at low voltages where the current is unsaturated (i.e., for $V < V_{\mathrm{p}}$). This line gives the electron temperature kT_{e} as 1.3 eV, and V_{p} and I_{e} are obtained directly from the "knee" of the plot as 3.5 V and 0.25 A, respectively. Using eq. 2, the mean electron speed is calculated to be $c_{\mathrm{e}} = 7.6 \times 10^5$ m/s, and using eq. 1, the electron density is calculated to be $n = 8.2 \times 10^{16}$ m^3. These are typical values for a glow discharge plasma [6]. The inset of Fig. 2b shows that for $V > V_{\mathrm{p}}$, the electron saturation current varies as $V^{1/2}$ due to the motion of electrons under the attractive positive potential of the cylindrical probe, in agreement with plasma probe theory [7]. The characteristic electron Debye length (λ) [6] of the plasma is given by

$$\lambda = \sqrt{\frac{\varepsilon_0 kT_e}{ne^2}} = 29\ \mu\text{m} \quad (4)$$

where ε_0 is the permittivity of free space.

The sheath width (S), assuming a typical Child's Law sheath [7], is given by

$$S = \frac{\sqrt{2}}{3}\lambda\left(\frac{2eV_0}{kT_{\mathrm{e}}}\right)^{3/4} = 2.3\ \text{mm} \quad (5)$$

where V_0 is the sheath voltage = V_{p} + 600 V = 603.5 V.

The magnitude of the electric field in the sheath is given by (4/3) × (603.5 V/2300 μm) = 0.35 V/μm, directed toward the cathode [7], and its extent is 2.3 mm, easily sufficient to encompass the growing nanotubes. The nanotubes, which are negatively biased at the cathode, experience a force opposite to the direction of the field (i.e., vertically upwards) at their tip, which guides them vertically during growth. The electric field strength we obtain here is in agreement with other published results [8].

ANALYSIS OF THE GROWTH MECHANISM DURING PLASMA-ENHANCED CHEMICAL VAPOR DEPOSITION

A detailed parametric study of the growth of carbon nanotubes by PECVD has been previously reported [9]. It was reported that the nanotube growth rate peaked at around 20 % C_2H_2 content, and it was shown that well-aligned nanotubes were grown for C_2H_2 concentrations between 4 and 20 %, that at 29 % C_2H_2 the nanotubes became more obelisk-like, and that by 38 % significant amorphous carbon was deposited (both on nanotube sidewalls and the substrate). At high C_2H_2 concentrations, amorphous

carbon gradually builds up on the nanotube as it grows upwards; as there is more amorphous carbon at the base, the nanotubes appear tip-shaped. These results are shown in Fig. 3.

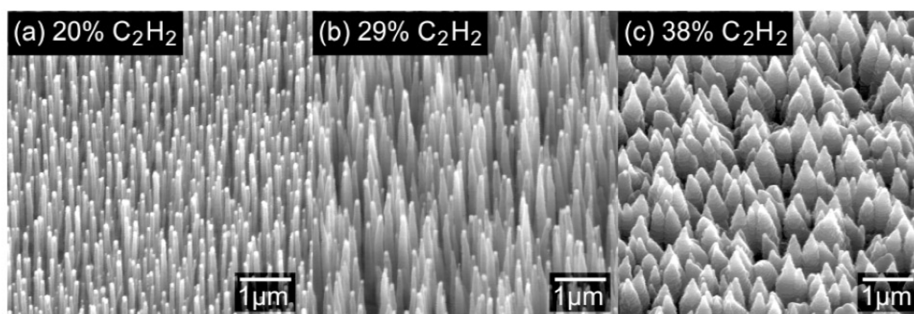

Fig. 3 Carbon nanotubes grown at different gas ratios.

In order to understand this, we conducted an analysis of the plasma composition during PECVD of carbon nanotubes [10] using an in situ mass spectrometer (Hiden EQP). The proportion of C_2H_2 in the NH_3:C_2H_2 plasma was varied between 0 and 70 % whilst maintaining other parameters at their standard settings (pressure 5 mbar, temperature 700 °C). Mass spectrometry was performed on species extracted 15 mm from the graphite stage. A mass spectrum for neutral species is shown in Fig. 4.

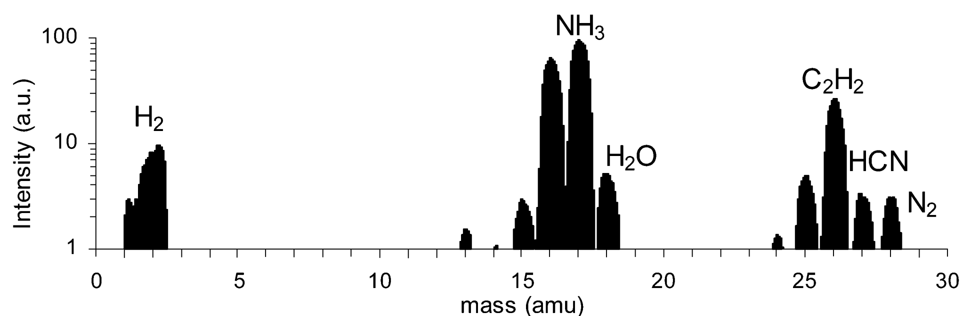

Fig. 4 Mass spectrum for neutral species.

The species in the spectrum are consistent with the cracking patterns of C_2H_2 and NH_3 and also indicate the presence of H_2, HCN, H_2O, N_2, and CO_2 [11]. This is consistent with data reported by other authors [12]. We did not detect C_2, CH_4, or other higher carbon species, even after long data acquisition periods. We therefore propose that C_2H_2 is the dominant precursor for nanotube formation, and will present more evidence to support this proposal later in this paper. This is supported by other authors [13] who have detected the presence of C_2H_2 in a $CH_4/H_2/NH_3$ plasma yielding nanotubes.

In order to understand why varying the gas ratio produces different structures, the role of NH_3 in the plasma is examined. The production of nanotubes requires a controlled deposition of carbon, which can then self-assemble into an energetically favored nanotube form. This controlled deposition rate is achieved through the combination of two reactions: the dissociation of a carbon-rich gas (in our case, C_2H_2) and the removal of excess carbon, which would otherwise lead to amorphous carbon deposits. It has been widely reported that atomic hydrogen is the active species for the removal of excess carbon. NH_3 has a key role in removing any excess carbon through the generation of reactive atomic hydrogen

species, which combine with and carry away carbon atoms. We can see the role of NH_3 in the level of H_2 detected in the plasma for varying gas ratio. This is shown in Fig. 5.

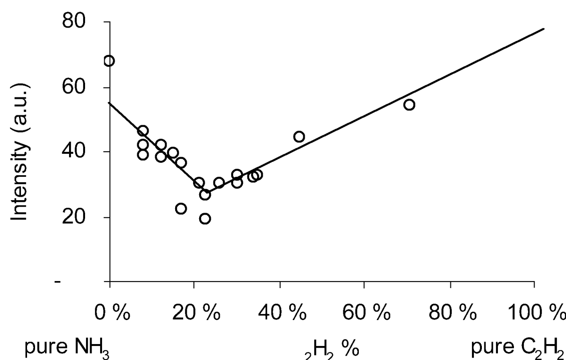

Fig. 5 H_2 signal for varying gas ratio.

H_2 is generated by the decomposition of both NH_3 and C_2H_2. To the left of the figure, where the plasma is predominantly NH_3, the amount of H_2 increases as NH_3 increases. In this region, the H_2 is derived from decomposition of NH_3. To the right of the figure, where the plasma is predominantly C_2H_2, the amount of H_2 increases as C_2H_2 increases. In this region, the H_2 is derived from the decomposition of C_2H_2.

At high NH_3 ratios, NH_3 decomposes preferentially over C_2H_2. This is because the chemical bonds that hold the NH_3 molecule together are weaker than those that hold C_2H_2 together. This allows the C_2H_2 to decompose slowly, generating the small amounts of carbon necessary for nanotube self-assembly. At high C_2H_2 ratios, there is insufficient NH_3 to effectively suppress C_2H_2 decomposition, resulting in higher levels of carbon generation and deposition of excess carbon as a-C. NH_3 therefore has two key roles in the formation of carbon nanotubes: Not only does it generate atomic hydrogen species to remove any excess carbon, it also suppresses the decomposition of C_2H_2, limiting the amount of carbon generated in the first place. The gas-phase removal of carbon-containing species results in the production of gaseous HCN, which is detected in the mass spectra of Fig 4.

Our observed minimum in H_2 is close to the previously reported peak in clean nanotube growth rate at around 20 % C_2H_2. At this ratio, carbon-removing species are at a minimum and C_2H_2 decomposition is low, giving rise to controlled deposition of clean nanotubes. Interestingly, ion intensities (see ref. [10]) were observed to peak at around 40 % C_2H_2, where a-C is deposited. The optimum condition for nanotube growth is, therefore, not the condition of maximum ion intensity. This contrasts with most thin film growth, where the condition with maximum ionization is preferred.

EFFECT OF PLASMA POWER ON GROWTH RATE

In order to investigate the effect of plasma power on the nanotube growth rate, nanotubes were grown at difference plasma powers whilst keeping the substrate/cathode temperature constant [14]. The conditions were the same in each case (substrate temperature 700 °C, chamber pressure 12 mbar, gas ratio 21 % C_2H_2), however, in one case the only source of heating was the plasma (200 W) and in the other a resistive heater was used to supplement the plasma heating (66 W). The results obtained in the two cases are shown in Fig. 6 below.

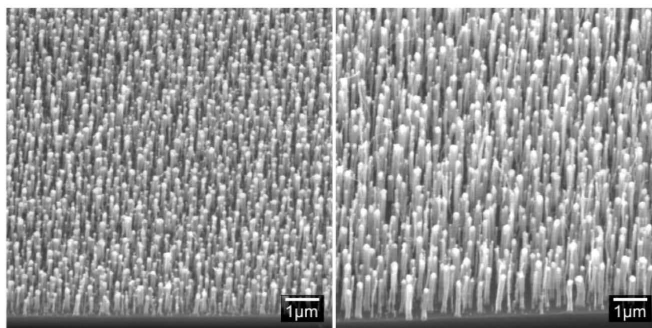

Fig. 6 Effect of varying plasma power. Power is 200 W on the left and 66 W on the right.

It is clear from this figure that increasing the plasma power has the effect of reducing the nanotube growth rate. The effect of the plasma on the decomposition of C_2H_2 is shown in Fig. 7. In our analysis of the growth mechanism, we proposed that the carbon atoms that form the nanotubes must be extracted from C_2H_2 in a reaction at the catalyst surface. We can see from Fig. 7 that as the plasma power increases, the decomposition of C_2H_2 also increases. This means that there is less C_2H_2 available to react with the catalyst particles to form the nanotubes, leading to the observed reduction in growth rate. For efficient growth of aligned nanotubes, we therefore need sufficient plasma power to generate the necessary electric field in the sheath region for nanotube alignment, but not so much as to dissociate large amounts of the carbon feedstock before it can reach the catalyst particles.

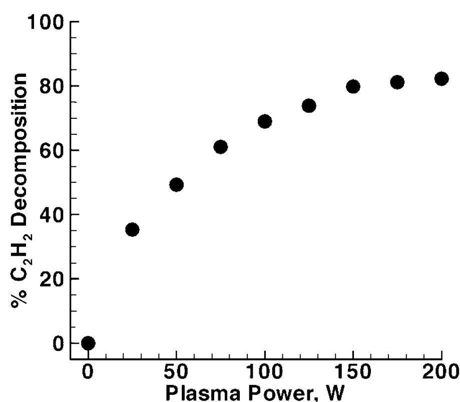

Fig. 7 Variation of gas decomposition with plasma power.

IMPORTANCE OF ENDOTHERMIC ION-MOLECULE REACTIONS

In order to investigate the reactions taking place inside the plasma, results from a 1-dimensional radially averaged computational model were compared with experimental measurements of species density. The model is discussed in detail in ref. [15]. The model included 21 neutral species, 7 charged species, and 200 reactions, including 15 exothermic ion-molecule reactions, and, unusually, 14 endothermic ion-molecule reactions. Endothermic reactions are not generally included in simulations as such reactions can only take place when ions have particularly high energies, however, in this case the high pressures and voltages involved mean that there is the potential for endothermic reactions to take place in the plasma sheath.

Unfortunately, whilst there is good published data on exothermic ion-molecule reaction rates, there is very little data regarding endothermic reaction rates. The data used for the endothermic reaction rates for both NH_3 and C_2H_2 were, therefore, approximated by the published rate for CH_4. Experimental data was recorded using the Hiden EQP plasma analyzer. Experimental measurements of NH_3 and C_2H_2 decomposition for varying plasma power were compared with the computational model both including and excluding the endothermic ion-molecule reactions, in order to assess their significance. These comparisons are shown in Fig. 8 below.

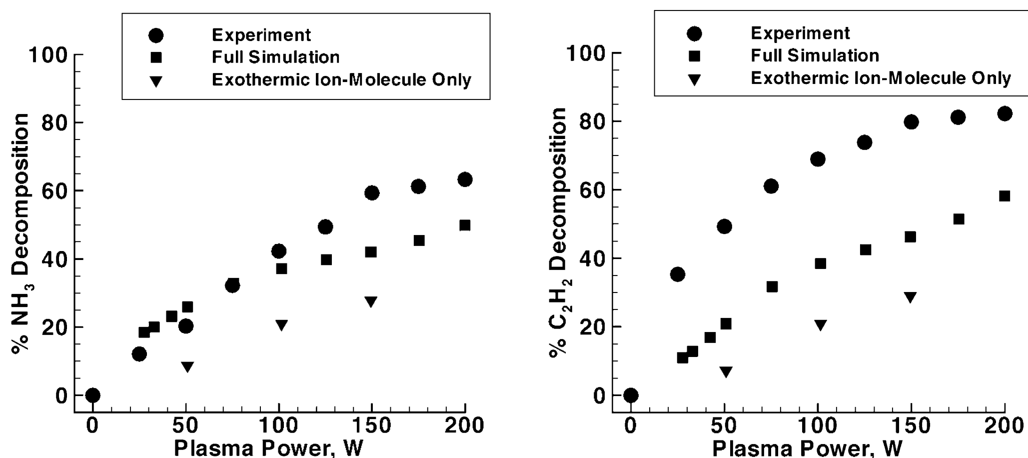

Fig. 8 Comparison of experimental and simulated data.

The first thing we notice is that in both cases the full simulation including the endothermic ion-molecule reactions provides a better fit than the simulation excluding endothermic reactions. This indicates that endothermic reactions are taking place to a significant degree within the plasma sheath. We can also see that the fit between simulation and experiment is better for NH_3, particularly at lower plasma powers where the fit is very good indeed. The discrepancy in the fit is likely to be due either to approximations in the analysis of the experimental data or errors in the rate estimates for the ion-molecule reactions. The rate estimates are the most probable source of error, as we used endothermic reaction rates for methane rather than acetylene or ammonia. It is likely that the rate for ammonia is closer to that for methane, which would explain the better fit for ammonia then for acetylene. Looking at the endothermic ion-molecule reactions in detail [15], the most important reactions are dissociative proton abstraction and collision-induced dissociation.

CONCLUSIONS

We have shown experimentally how the use of a dc plasma during CVD of carbon nanotubes aligns the nanotubes in the direction of the electric field, and have determined the magnitude and extent of this field. The dual role of NH_3 in both suppressing the decomposition of the carbon feedstock and removing excess carbon to prevent the formation of amorphous carbon during PECVD has been examined. The effect of varying the plasma power has been investigated, and the reduced growth rate at higher plasma powers is explained by the increased decomposition of C_2H_2 at high plasma powers. This result confirms our proposition that C_2H_2 is the dominant precursor for carbon nanotube growth in this process. Finally, we have shown the importance of endothermic ion-molecule reactions in the plasma sheath by comparing measured data with simulation results. Overall, we have provided a number of in-

sights into the chemical and physical processes underlying the growth of vertically aligned carbon nanotubes by PECVD.

ACKNOWLEDGMENTS

M. S. B. acknowledges support from the Engineering and Physical Sciences Research Council. K. B. K. T. acknowledges the support of the Royal Academy of Engineering and Christ's College Cambridge. Some of this work and ISPC conference cost was supported through EC FP6-STREP DESYGN-IT.

REFERENCES

1. S. Ijima. *Nature (London)* **354**, 56 (1991).
2. C. Journet, W. K. Maser, P. Bernier, A. Loiseau, M. L. delaChapelle, S. Lefrant, P. Deniard, R. Lee, J. E. Fischer. *Nature* **388**, 756 (1997).
3. A. Thess, R. Lee, P. Nikolaev, H. J. Dai, P. Petit, J. Robert, C. H. Xu, Y. H. Lee, S. G. Kim, A. G. Rinzler, D. T. Colbert, G. E. Scuseria, D. Tomanek, J. E. Fischer, R. E. Smalley. *Science* **273**, 483 (1996).
4. V. I. Merkulov, D. H. Lowndes, Y. Y. Wei, G. Eres, E. Voelkl. *Appl. Phys. Lett*. **75**, 1086 (1999).
5. K. B. K. Teo, M. Chhowalla, G. A. J. Amaratunga, W. I. Milne, G. Pirio, P. Legagneux, F. Wyczisk, J. Olivier, D. Pribat. *J. Vac. Sci. Technol.* **20**, 116 (2002).
6. B. N. Chapman. *Glow Discharge Processes*, pp. 49–82, John Wiley, New York (1980).
7. M. A. Lieberman, A. J. Lichtenberg. *Principles of Plasma Discharges and Materials Processing*, pp. 164–166, John Wiley, New York (1999).
8. Y. Zhang, A. Chang, J. Cao, Q. Wang, W. Kim, Y. Li, N. Morris, E. Yenilmez, J. Kong, H. Dai. *Appl. Phys. Lett.* **79**, 3155 (2001).
9. M. Chhowalla, K. B. K. Teo, C. Ducati, N. L. Rupesinghe, G. A. J. Amaratunga, A. C. Ferrari, D. Roy, J. Robertson, W. I. Milne. *J. Appl. Phys*. **90**, 5308 (2001).
10. M. S. Bell, R. G. Lacerda, K. B. K. Teo, N. L. Rupesinghe, M. Chhowalla, G. A. J. Amaratunga, W. I. Milne. *Appl. Phys. Lett*. **85**, 1137 (2004).
11. NIST Chemistry WebBook, <http://webbook.nist.gov/>.
12. B. A. Cruden, A. M. Cassell, Q. Ye, M. Meyyappan. *J. Appl. Phys.* **94**, 4070 (2003).
13. Y. S. Woo, D. K. Jeon, I. T. Han, N. S. Lee, J. E. Jung, J. M. Kim. *Diamond Relat. Mater.* **11**, 59 (2002).
14. K. B. K. Teo, D. B. Hash, R. G. Lacerda, N. L. Rupesinghe, M. S. Bell, S. H. Dalal, D. Bose, T. R. Govindan, B. A. Cruden, M. Chhowalla, G. A. J. Amaratunga, M. Meyyappan, W. I. Milne. *Nano Lett.* **4**, 921 (2004).
15. D. B. Hash, M. S. Bell, K. B. K. Teo, B. A. Cruden, W. I. Milne, M. Meyyappan. *Nanotechnology* **16**, 925 (2005).